Indian Journal of Engineering & Materials Sciences
Vol. 28, August 2021, pp. 393-408

Effects of iron powder on properties of geopolymers subjected to different curing regimes

Nihan Gulmez[a]*, Niyazi Ugur Kockal[b]

[a]Department of Civil Engineering, Munzur University, 62000, Tunceli, Turkey

[b]Department of Civil Engineering, Akdeniz University, 07058, Antalya, Turkey

Received: 12 September 2020; Accepted: 5 July 2021

Silica fume, slag and iron powder are by-products from various industries. In parallel with development of industrial technology, it is also known that these by-products which cause rapid pollution of the environment are also harmful to human health because they are easily respirable. For this reason, a series of experiments were carried out to determine physical and mechanical properties on samples prepared using different blend designs to examine the effect of factors such as curing conditions, binder type and waste iron powder content. Percentages of iron powder added to replace the aggregate are 10%, 20%, 30% and 40% by volume of slag aggregate. It was observed that the substitution of 30% by volume iron powder instead of slag in geopolymer mortars is the most effective in increasing splitting tensile strength. For 40% partial replacement of fine aggregates with iron powder, increases in compressive strength and flexural strength of slag-based mortars were 7.2% and 43.4%, respectively, compared to mortar without iron powder at 60°C curing conditions.

Keywords: Geopolymer, Iron powder, Silica fume, Slag

1 Introduction

The contribution of Ordinary Portland Cement (OPC) production in greenhouse gas emissions worldwide is known. Thus, it has been suggested that there is a need for the use of fewer natural sources and the need for OPC alternatives that require less energy source (CO_2) to reduce the environmental impact of concrete production[1-3]. As an approach for this purpose, OPC is completely replaced by the by-product materials such as ground-granulated blast-furnace slag obtained after a series of metal extraction processes, fly ash produced from the burning coal[4-6]. As a result, a new material is produced by combining fly ash, slag, silica fume and other natural wastes and it is called geopolymer[7-12]. One of main features of geopolymer is that it is an environmentally friendly alternative providing low energy consumption and waste consumption due to its use of waste or by-products compared to other materials[13]. Alumino-silicate binders are called inorganic geopolymer compounds because of the fact that they are obtained as a result of inorganic polycondensation rection defined as geopolymerization[14]. SiO_4 and AlO_4 tetrahedra chained by sharing oxygen atoms generate a sialate network. Charges neutralized with monovalent cations Na^+ and K^+ and located on alumina tetrahedral units are negative charges[15]. Geopolymers, which have excellent physical and mechanical properties, gain an advantage over other cement-based materials[16]. Also, NO_x, SO_x, CO, and CO_2 don't occur in geopolymer in comparison with Portland cement[17]. New generation materials including molecular chains and/or 3-D silico aluminate (Si-O-Al) amorphous structures that are covalently bonded, have been named geopolymers[18]. Recently, there has been a growing interest in geopolymers with excellent properties such as freeze-thaw resistances, corrosion resistance, low environmental impact, good mechanical properties, low shrinkage, permeability resistance, cost efficiency, high early-age strength gain, acid and sulfate resistance, fire resistance[19,20]. It was reported that source material characteristics such as fineness, chemical composition, particle size distribution, and reactive silica and alumina amount in geopolymer precursors considerably affect strength and stability of geopolymer[21]. In addition, factors such as water content, pH range, concentration and type of alkaline solutions, and pH level are also very important on the behaviour of geopolymer[22-24]. The workability and rheology of geopolymer mortars based on slag and fly ash were investigated by Alanso[25] to research effects

*Corresponding author (Email: nihangulmez@munzur.edu.tr)

of alkaline activator type, activator concentration, aggregate content and precursor materials. The effect of adding a finer material than portland cement on the workability of mixtures can be explained by two main phenomena[26]. The first is the improvement of packing density: fine particles fill voids, releasing excess water, resulting in an increase in workability[27]. Another phenomenon is the increase in surface area, which reduces the thickness of the water film over which solid particles are coated[28]. For higher surface areas, the same amount of water film will be thinner and the flow capacity will be reduced[29-30]. Depending on which of these two phenomena, defined as the effect of improving the packing density or the effect of increasing the surface area, dominates, the effect of silica fume on workability is clearly directed[31]. In different studies, it was reported that the workability of mixtures is improved at low silica fume contents and decreased at higher amounts[32-33]. It was reported by Srivastava *et al.*[34] that silica fume significantly increases the workability and strength of mixtures and the optimum replacement ratio with portland cement is 5% by weight. In another study by Duval and Kadri[35], it was observed that silica fume can replace 10% cement without harming concrete workability. In mixtures without superplasticizers, fine particles will agglomerate, increasing the water requirement as they cannot fill voids between larger particles, so it is generally practical to compensate for the decrease in workability in silica fume-cement based mixtures by adding chemical additives or adjusting the water/cement ratio[36-37]. It was reported that, in contrast to the increased cohesion in concrete due to the ultrafineness of silica fume, which is known as a highly reactive pozzolanic material, the high amount of water required to maintain the desired workability can be balanced with the addition of superplasticizer[38].

The effect of replacement of slag with 5%, 10% and 15% silica fume on compressive strength of slag-based geopolymer concrete was investigated and it was seen that 28 and 90 days compressive strength of samples containing silica fume were higher than those of samples without silica fume[39]. Collins and Sanjayan[40] examined the effect of silica fume on the workability and strength development of slag-based geopolymer concrete. They reported that the compressive strength of concrete sample prepared by replacement of slag with 10% silica fume was found to be 74.2 MPa for 91 days and it was stated to be 12% higher than the strength of slag-based concrete. In order to determine the permeation properties of geopolymer concrete, the water absorption capacity, apparent porosity and volume ofpermeable voids of the geopolymer concrete were investigated[41]. The experimental data showed thatcompared to the equivalent control concretes of geopolymer concrete samples, water absorption capacity and volume of permeable voids decreased by 38.38%, 37.62%, respectively. In the study carried out by Das *et al.*[42] on geopolymer concrete containing fly ash and blast furnace slag, it was observed that the increased substitution of rice husk ash reduced the compressive strength and workability. Katpedy *et al.*[43] investigated performance of slag based geopolymer prepared with a pyroclastic flow deposit (Shirasu) as aluminosilicate source. As a result, it was reported that initial and long term strength and resistance to acid of Slag-Shirasu geopolymer improved with increasing amount of slag. Strain-hardening geopolymer composite containing fly ash and slag with a low slag content was aimed to be developed using a micromechanical model to control design of mixtures, and it was obtained composites having 4.8% tensile strain capacity and ultimate tensile strength above 3.8 MPa[44].

It was observed by Zhu *et al.*[45] that freezing resistance and strength of slag-based geopolymer with the addition of modified flyash significantly increased owing to the filling functions of active agents (β-C_2S and C_3S), compared to geopolymer produced with the inclusion of original fly ash. In ultra-high toughness geopolymer samples produced with fly ash and steel slag by Guo and Yang[46], they observed that curing at high temperature increased the strength of geopolymer while reducing its compactness and strain properties. The microstructure and early mechanical properties of metakaolin-based geopolymers prepared with the replacement of 20% and 40% slag instead of metakaolin were investigated on samples submerged in the karst water used as corrosive solution[47]. It was reported that with the reduction of slag in mixtures, samples showed greater resistance toward corrosion of karst water. Effects of the type and amount of alkali activators besides the slag amount on geopolymers produced by replacing the fly ash with slag (CaO-rich material) were investigated by Oderji *et al.*[48]. Experimental results showed that more than 8% Na_2SiO_3 amount as activator and more than 15% slag as substitution in the geopolymer provide more reacted particles.

Li *et al.*[49] observed that a new green material produced with partial replacement of cement or fine sands with iron ore powder in foamed concrete has good physical and mechanical properties and it can also decrease environmental pollution arising from waste metal. Shishegaran *et al.*[50] investigated concrete made with steel powder and steel wire rope to enhance mechanical and conductive properties and to solve environmental problems thanks to the reuse of waste. They reported that they achieved the desired values of compressive strength and electrical resistivity with the optimum combination ratio of steel powder and wire rope. The effect of aluminium powder fineness on properties of aerated cement paste and mortar such as compressive strength, fresh density, workability, dry density, aeration rate, water absorption was examined by Kumar and Ramamurthy[51].

In view of researches in the literature, some studies focused on the effect of using various waste metal materials such as aluminium powder, steel powder, iron ore tailings on properties of conventional Portland cement mortar/concrete. But there is little research on the geopolymer used iron powder for silica fume based mortar yet. In addition, most studies focus on geopolymers produced with products such as metakaolin, fly ash, rice husk ash, while effects of silica fume on geopolymer still expect to shed light on them.

Considering that the literature in this subject is rather poor, there is a need for further investigation. The main aim of the this study is to investigate properties of eco-friendly mortars with high-volume of silica fume and iron powder. In order to reach this purpose, experiments determining physical, mechanical and durability properties such as bulk density, apparent porosity, water absorption, tensile strengths, compressive strengths and sorpivity were carried out. In contrast to previous studies, silica fume was used at high replacement levels up to 60% in conjunction with slag. In addition, this paper focuses on evaluating how different curing conditions can control properties of geopolymer with different binder and aggregate ratios by keeping the alkali activator solution constant.

2 Materials and Method

2.1 Raw materials

Binder precursors used in the preparation of geopolymer mortars are slag and silica fume as main sources of silica (SiO_2) and alumina (Al_2O_3) and their specific gravities are 2.815 and 2.275, respectively. The particle size distribution and specific surface area of precursors used as binders are given in Table 1. Apart from slag used as binder, a different type of slag sourced from another a local steel-making plant was introduced to replace the fine aggregate in the mixture. Chemical compositions of silica fume and slag materials are given in Table 2. Fine aggregates used in mixtures consisted of two different types of aggregate as slag with a specific gravity of 3.03 besides a fineness modulus of 4.16 and iron powder with a specific gravity of 6.78 besides a fineness modulus of 3.33. Results of sieve analysis of fine aggregates are given in Fig. 1. Sodium silicate (Na_2SiO_3) and sodium hydroxide (NaOH) were used as alkali activation solutions. The purity of NaOH in pellet form is more than 98% and its molecular weight is 40 g/mol. By dissolving sodium hydroxide pellets in distilled water, a sodium hydroxide solution of 8 molar (M) concentration was prepared. The specific gravity of the solution, which was rested for 24 hours

Table 1 — Particle size distribution and specific surface area of silica fume and slag

Materials	Specific surface area (m^2/g)	Particle size distribution (μm)		
		d(0.1)	d(0.5)	d(0.9)
Silica fume	2.79	0.766	5.479	12.351
Slag	1.87	1.251	9.013	24.282

Table 2 — Chemical compositions of constituents (%)

Oxide	Silica Fume (binder)	Slag (binder)	Slag (aggregate)
Na_2O	2.15	1.13	1.39
MgO	14.32	7.725	10.64
Al_2O_3	1.684	15.04	9.343
SiO_2	78.02	31.44	13.09
P_2O_5	0.02396	-	-
SO_3	0.2984	0.3434	0.1752
Cl	0.02678	0.02592	0.02091
K_2O	1.097	0.4024	-
CaO	0.1931	41.92	56.49
TiO_2	-	0.5262	0.04413
Cr_2O_3	1.405	-	6.392
MnO	0.0560	0.5138	0.072
Fe_2O_3	0.3170	0.5862	1.218
CuO	-	0.0863	-
ZnO	0.1950	-	-
SrO	-	0.09554	0.02081
ZrO_2	< 0.068	< 0.068	< 0.068
Ba	-	0.1218	-

after preparation, was found to be 1,236. Chemical values for Na_2SiO_3 are given as SiO_2/Na_2O=2, Na_2O%=14.9, SiO_2%=29.8. The specific gravity of sodium silicate is 1,425. Combinations prepared by mixing silicate, hydroxide and other source materials are described in Table 3. To ignore the effect of the activation solution on the performance of slag/silica fume-based geopolymer mortars, four types of mortar (SF0-I, SF20-I, SF40-I, SF60-I) were produced using the same volumetric ratio (1:1) of hydroxide and silicate.

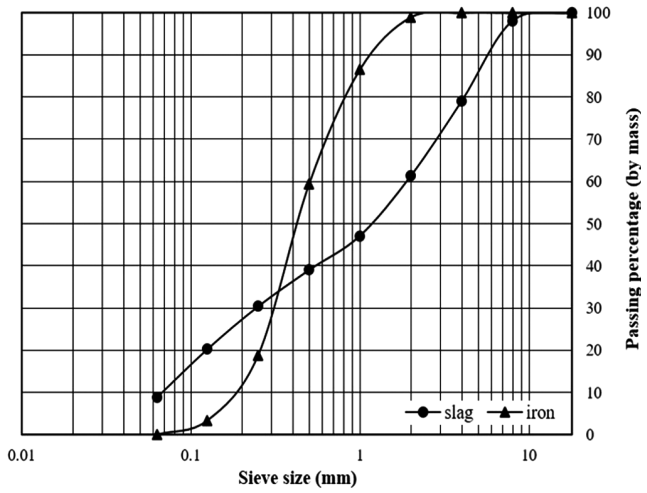

Fig. 1 — Sieve analysis of slag and iron powder aggregates.

2.2 Preparation of geopolymers

Silica fume-slag based geopolymers were produced according to following procedure. Sodium hydroxide solution prepared at 8 molar concentration was used after resting for 24 hours. Initially, hydroxide and silicate as alkali-activating solutions were mixed with each other. Later, aggregates were mixed in the mixer with the alkaline activating solution for 1 minute. While the resulting mixture was stirred in the mixer at a low speed, binders were added gradually to the mixture for 1 minute. The mixture was then homogenized for 1 minute at high speeds in the rotary mixer. Fresh mortars obtained at the end of this processes were poured to the mold and these molds were subjected to vibration in order to provide settlement. Samples were removed from molds after 24 hours, and each of equivalent mortars produced for different curing conditions were stored for 48 hours at two different water temperatures of 23°C and 60°C (by exposing them at temperatures that only concern themselves). Curing temperatures of 23°C and 60°C are coded as CT-23 and CT-60 in graphs presenting the experimental data, respectively.

2.3 Physical and mechanical tests

The bulk density, absorption and apparent porosity values were obtained on 40x40x160 mm

Table 3 — Volumes of materials used in the preparation of geopolymers

Series Code	Mix Code	Na_2O_3	NaOH solution	Slag binder	Silica fume binder	Slag aggregate	Iron powder aggregate
SF0-I	SF0	175	175	200	-	450	-
	SF0-I10	175	175	200	-	405	45
	SF0-I20	175	175	200	-	360	90
	SF0-I30	175	175	200	-	315	135
	SF0-I40	175	175	200	-	270	180
SF20-I	SF20	175	175	160	40	450	-
	SF20-I10	175	175	160	40	405	45
	SF20-I20	175	175	160	40	360	90
	SF20-I30	175	175	160	40	315	135
	SF20-I40	175	175	160	40	270	180
SF40-I	SF40	175	175	120	80	450	-
	SF40-I10	175	175	120	80	405	45
	SF40-I20	175	175	120	80	360	90
	SF40-I30	175	175	120	80	315	135
	SF40-I40	175	175	120	80	270	180
SF60-I	SF60	175	175	80	120	450	-
	SF40-I10	175	175	80	120	405	45
	SF40-I20	175	175	80	120	360	90
	SF40-I30	175	175	80	120	315	135
	SF40-I40	175	175	80	120	270	180

prism samples in accordance with ASTM C 642-06[52].

Splitting tensile strength tests of mortars were performed on 50x100 mm cylindrical samples in accordance with TS EN 12390-6[53]. The load was applied continuously until the sample broke at a constant speed of 0.5 kN/s. Flexural and compressive strengths of hardened mortar samples were determined in accordance with TS EN 196-1[54]. Flexural strengths of mortars were determined by loading 40x40x160 mm prism samples from three points and each part of fractured samples was used for the determination of compressive strength.

Capillary water absorption tests were applied on samples dried at 80°C in an oven for 48 hours after curing in accordance with TS EN 480-5[55]. Samples were covered with paraffin to prevent water absorption from other surfaces, except for bottom surface which is immersed 2-3 mm under the water. The amount of water absorbed by the capillary was measured by weighing samples after 24 hours. Sorptivity coefficients of mortars were determined according to Eq. 1.

$$k_c = (Q/A)^2 x 1/t \quad \ldots (1)$$

where, Q is the amount of water suction, A is the cross-section of mortarscontacting with water and t is the exposure time.

3 Results and Discussion

3.1 Physical properties

3.1.1 OD bulk density

OD bulk density graphs of mix series are shown in Fig. 2. Results showed that for 10% ratio of iron powder in mortar (SF0-I10), the increase in the bulk density was about 6.2% compared to slag-based mortars without iron powder (SF0) at CT-23 curing condition. It was also observed that substitution of up to 40% of fine aggregates by volume with iron powder in mortars resulted in an increase of 25.1% in bulk density of mortars at CT-23. Similar results were also observed for CT-60 conditions that increases in bulk density of mix designs SF0-I10 (10% iron powder) and SF0-I40 (40% iron powder) were 6% and 22% respectively, compared to mortars without iron powder (SF0). This result is thought to be due to the fact that the iron powder substitute with a higher specific gravity of 6.78 compared to the slag with a specific gravity of 3.03 increases bulk densities of mortars. The increase in the bulk density of SF40-I40

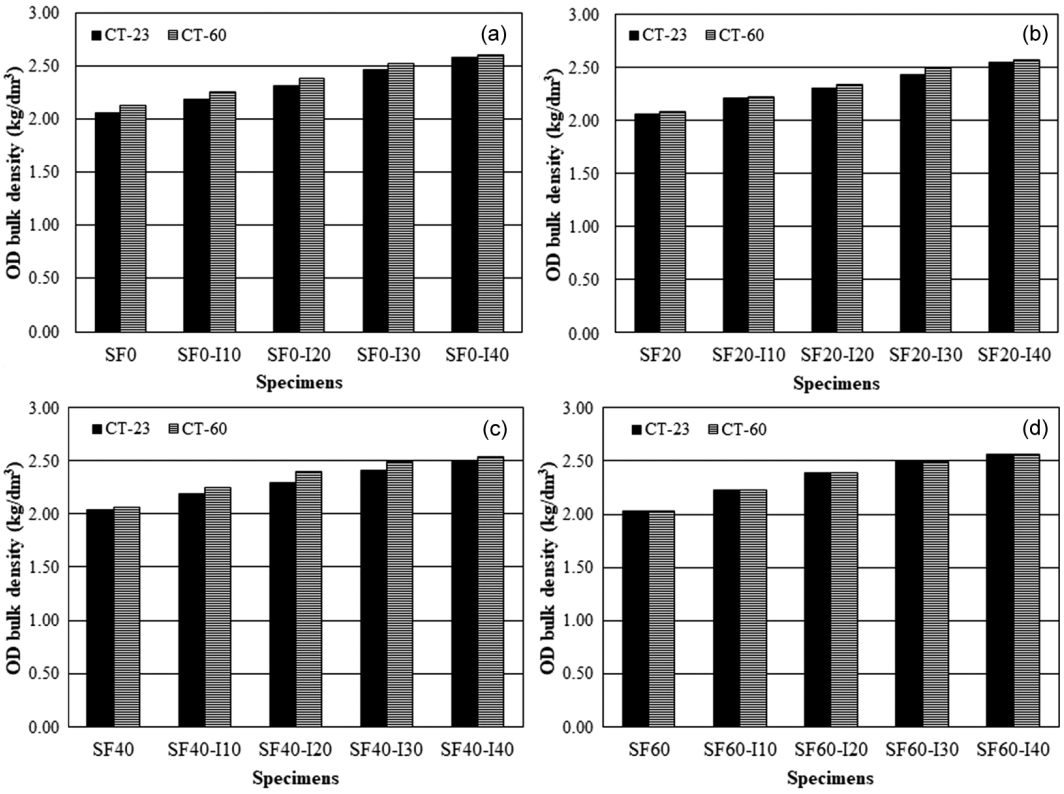

Fig. 2 — OD bulk density for a) SF0-I, b) SF20-I, c) SF40-I, and d) SF60-I series.

containing iron powder as fine aggregates replacement at level of 40%, by volume was approximately 23.3% in comparison with control specimen (SF40) at CT-60. Among all mortars that do not contain iron powder SF0 exhibited the highest bulk density values of 2.06 kg/dm^3 (at CT-23) and 2.13 kg/dm^3 (at CT-60). This may be due to a spherical shaped, high-fine silica fume with a relatively low specific gravity to the slag, resulting in a reduction in bulk density. Using silica fume at level of 60%, by volume in mortars gave the lowest bulk density of 2.02 kg/dm^3(CT-23) ve 2.03kg/dm^3 (CT-60). Cheah and Ramli[56] expressed that silica fume is commercially provided in densified form on account of the fact that undensified silica fume has low bulk density causing problem in transportation of the material. They also reported that densification in order to increase bulk density of silica fume leads to agglomeration and thus its hydration and microfiller properties might be influenced with changing particle size and distribution. Based on this study, it can be extrapolated that the amount of silica fume in mortar and curing conditions have a significant effect on the bulk density of hardened mortars. There was a general tendency to significantly decrease bulk density with increasing silica fume replacements.

3.1.2 SSD bulk density

Figure 3 presents SSD bulk density of mortars. In both curing conditions, SSD bulk density of all samples increased with increasing iron powder content. SSD bulk density of mortars (SF0-I10) containing 10% iron powder increased by 5.7 % (CT-23) and by 6.3% (CT-60) compared to the control (SF0). Results showed higher bulk density with increasing of curing temperature. This can be explained by the increase in the amount of hydration products in parallel with the increase in the curing temperature. The high temperature factor may have resulted in an increase in bulk densities by accelerating hydration and causing an increase in the amount of product at the exit of the reaction and a denser composition. SSD bulk density of SF20-I30 containing 30% iron powder by volume was also 15.3% higher than control mortars (SF20) which are without iron powder at CT-23. SF40 mortars showed SSD bulk density values of 2.307 kg/dm^3 (CT-23) and 2.315 kg/dm^3 (CT-60). Silica fume as partial replacement in mortars reduced values of SSD bulk density and the lowest bulk density values were obtained with mortars having the highest silica fume content (SF60) among all mortars as 2.29 kg/dm^3 (CT-23) and 2.30 kg/dm^3 (CT-60). This indicates a

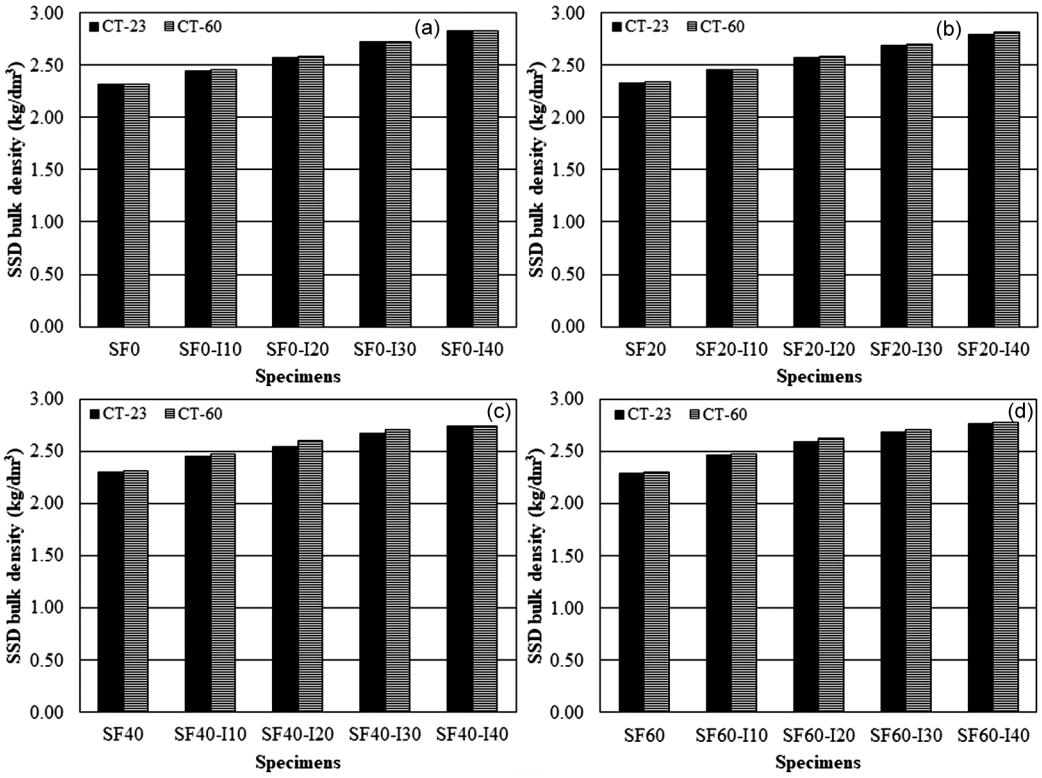

Fig. 3 — SSD bulk density for a) SF0-I, b) SF20-I, c) SF40-I, and d) SF60-I series.

higher specific gravity of slag relative to silica fume, similar to OD bulk density results. As a result, the reduction in the density of mortar components will also reduce bulk densities of mortars produced. Results showed the prepared mortars with partially replacement of 40% iron powder with fine aggregates and 60% silica fume content (SF60-I40) indicated the same increase of 20.9% in bulk density compared with control mortars (SF60) at both curing conditions. In addition, the partial replacement of 40% iron powder with fine aggregates (SF40-I40) led to an increase of 18.7% in SSD bulk density as compared to SF40 at CT-60. Results showed the addition of iron powder to mortars leads to an increment in SSD bulk density and that a high iron powder content was accompanied by a high increase in bulk density. The high percentage increase observed in bulk densities is a result of the substitution of iron powder as the metal component, which has a much higher specific gravity than the slag aggregate.

3.1.3 Water absorption

Figure 4 shows water absorption values of mixture series. Among SF0-I mixture series, SF0 has the highest water absorption values of 12.3% (CT-23) and 9% (CT-60), whereas SF0-I30 has the lowest values of 10.1% (CT-23) and 8.2% (CT-60). In this study, the water absorption percentage of slag aggregate was determined as 4.263%, it is thought that the metal component iron powder, which is replaced by slag as fine aggregate, does not absorb water and does not hold water on the surface. Therefore, the decrease in water absorption values can be attributed to the addition of metal component. These results are in accordance with findings in cement mortars reported by Miah *et al.*[57]. They observed that porosity and water absorption of specimens produced with replacement of 30% natural sand by recycled iron powder decreased by 36% and 48%, respectively, in comparison with specimens made with 100% natural sand. Shettima *et al.*[58] investigated concrete including the addition of iron ore tailings (25%, 50%, 75% and 100%) to replace river sand, with w/c ratio of 0.5. They pointed out that water absorption values of concrete containing iron ore tailings were lower than compared to control specimen. Authors also reported that the increase of curing period reduced water absorption because of iron ore tailings fineness and the development of hydration process. The concrete produced with synthetic gravel derived from recycled

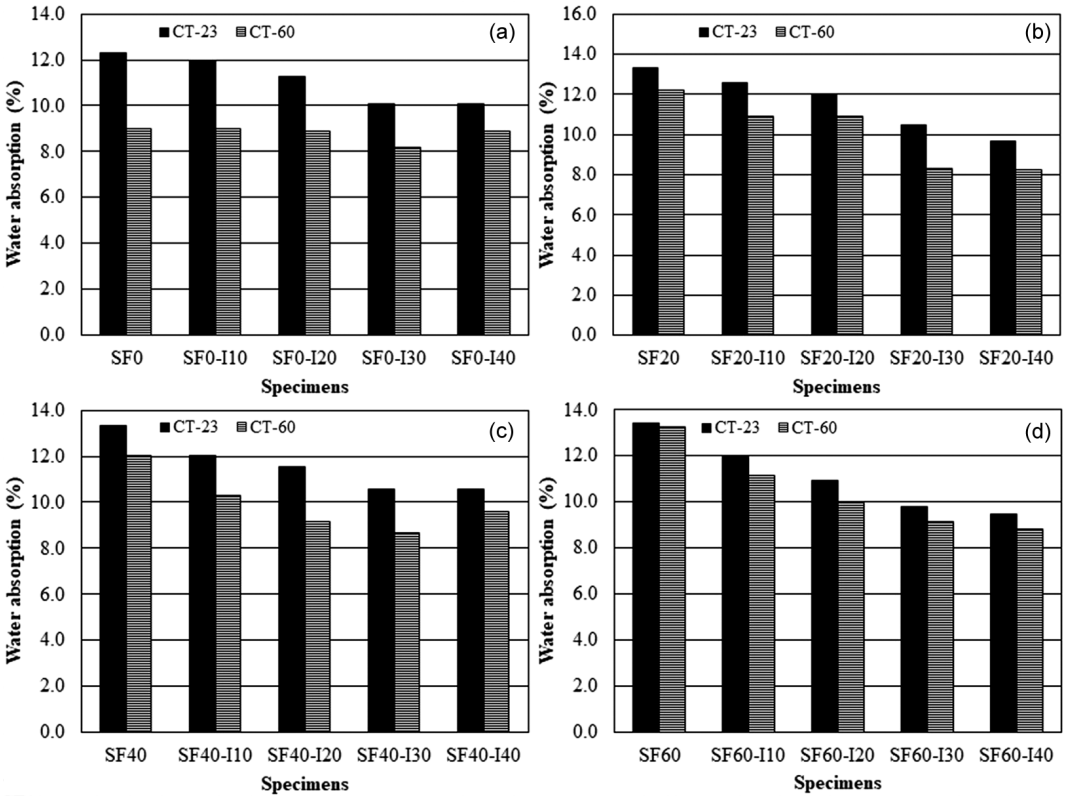

Fig. 4 — Water absorption for a) SF0-I, b) SF20-I, c) SF40-I, and d) SF60-I series.

polyhydroterphatalate and iron ore tailings had 1.9 g/cm^3 dry density, 15% water absorption and 27% void ratio[59]. Yunhong *et al.*[6] indicated that the incorporation of activated siliceous iron tailings (10%, 20% and 30%) led to an increase in impermeability of concrete; however, it was observed a decrease in impermeability with the use of 40% iron tailings.

SF20 produced by replacing 20% silica fume with slag gave water absorption of 13.4% at CT-23. However, further increase in SF content from 20 to 60% had insignificant effect on water absorption which showed almost a constant value of 13.4% until the amount of 60% silica fume. Sasanipour *et al.*[61] emphasized that silica fume used in mixtures can decrase water absorption and porosity. They also explained that with the inclusion of 25% and 50% silica fume, water absorption reduced by 32% and 18%, respectively, compared to non-silica fume mixtures. Of all mortars, SF60 showed the highest water absorption of 13.2% at CT-60. This can be explained by excess water holding capacity of the silica fume caused by its high specific surface and high fineness. In addition, results of the study show that mortars produced with high percentages of silica fume substituted with slag have a more porous structure, so it can be said that the increase in the apparent porosity causes an increase in the water absorption capacity. The increasing of curing temperature positively affected values of water absorption by resulting in a reduction significantly. In this case, water absorption values of SF40-I30 were 10.6% and 8.7% at CT-23 and CT-60, respectively. In other words, the reduction of 17.9% in water absorption of SF40-I30 recorded between CT-23 and CT-60 conditions of curing. This result can be explained by the decrease in water absorption values due to the dense structure obtained as a result of the improvement of hydration process with the increase in the curing temperature.

3.1.4 Apparent porosity

Graphs in Figure 5 show apparent porosity. SF20 and SF60-I40 mortars among all combinations for geopolymer mortars in this study exhibited a maximum apparent porosity of 27.8% and a minimum apparent porosity of 24%, respectively, at CT-23. This indicates that the increased porosity with silica fume substitution can be compensated for with iron powder. It is thought that the dense porous structure in the mortar, due to the high substitution ratios of

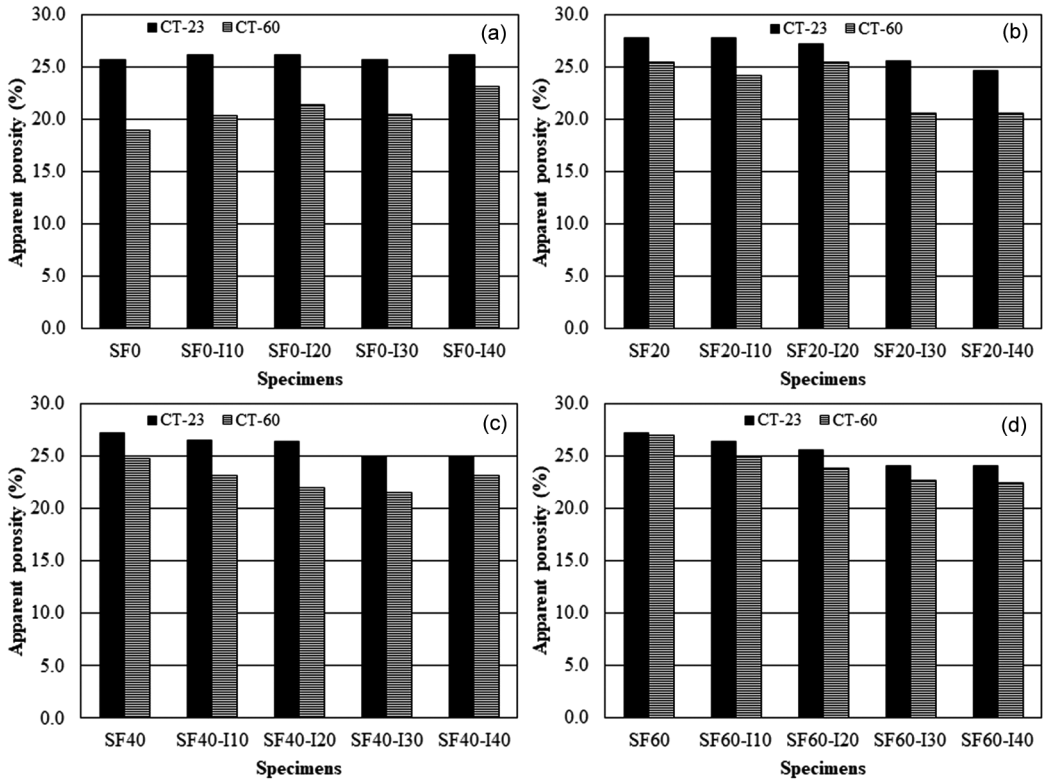

Fig. 5 — Apparent porosity for a) SF0-I, b) SF20-I, c) SF40-I, and d) SF60-I series.

silica fume with high fineness, may be clogged with a kind of filling function thanks to the iron powder with a uniform shape and finer aggregate diameter than slag aggregate, thus reducing the porosity. However, at CT-60, values of highest apparent porosity (26.9%) and lowest apparent porosity (18.9%) were obtained with SF60 and SF0, respectively. This situation revealed the importance of curing temperature effect. A significant increase in workability was observed with 60% silica fume substitution for slag. Consequently, the porosity left behind by the loss of excess water evaporated by bleeding is thought to be too large to be compensated by curing temperature. Furthermore, the inclusion of iron powder contributed to reduce apparent porosity of mortars at both curing conditions. For example, in series of SF60, the apparent porosity of mortars including 40% iron powder was less than reference mortars not containing iron powder. Result from this study is in concordance with others previous research on cement-based concrete. Largeau *et al.*[62] also observed that replacing 1.5 % and 2.5%, by weigth, portland cement by iron powder decreased porosity by 21.88% and 26.77%, respectively. They also concluded that the use of iron powder particles (Fe_2O_3) could significantly improve properties of concrete.

The addition of silica fume to mixture of metakaolin-based geopolymer foams caused an increase in the percentage of porosity. However, it was observed that the trend in compressive strength differed from that of porosity, and geopolymer containing silica fume of 5% gave the best performance[63]. In ultra-high performance samples prepared by using iron ore tailings instead of natural aggregate, it was observed that the threshold pore size was not significantly affected but the total porosity increased as wastes were incorporated[64]. They also verified the dilation of micro-pore structure of the material and the relation between the porosity and compressive strength. However, in this study, it was observed that the finer sized iron powder compared to the normal slag aggregate had a significant effect on the performance of mortars by providing filling function in the porous structure and improving the macro structure. SF20 exhibited the highest apparent porosity values recorded by 27.8% (CT-23) ve 25.4% (CT-60), whilst SF20-I40 showed the lowest apparent porosity values found by 24.6% (CT-23) and 20.6% (CT-60).

3.1.5 Sorptivity coefficient

Figure 6 exhibits the sorptivity coefficients of mixture series. It can be said that there was a tendency to decrease sorptivity coefficient with increasing in the percentage of iron powder for all mortars of SF0-I,

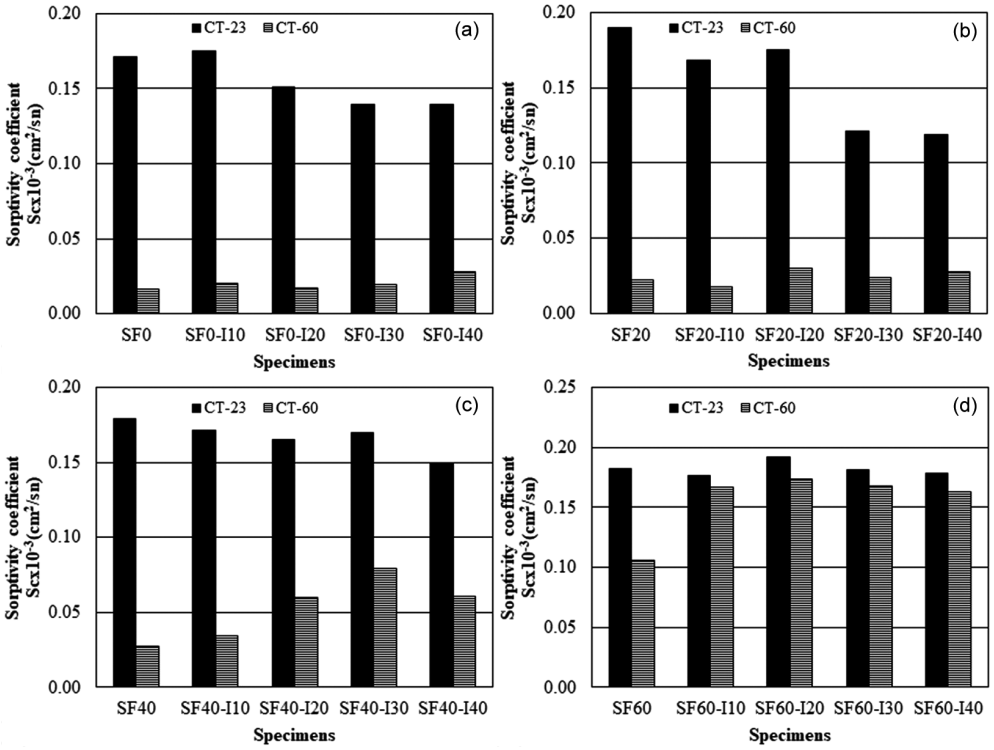

Fig. 6 — Sorptivity coefficient for a) SF0-I, b) SF20-I, c) SF40-I, and d) SF60-I series.

SF20-I ve SF40-I series at CT-23 conditions. However, it was observed that 60% silica fume as a partial replacement for binder has no significant influence on the sorptivity at CT-23. Adil *et al.*[65] stated that best results in relation to durability, phsical and mechanical properties were achieved by adding silica fume of 5%. However, more than 5% silica fume substitution was reported to result in a decrease in durability due to an increase in the content of void. This was attributed to the loss of controlled behavior of the load-bearing material as a result of increased silica fume. Furthermore, the increase of curing temperature from 23°C to 60°C significantly affected sorptivity of mortars, and the maximum sorptivity coefficient values were obtained with SF0-I40 ($0.03x10^{-3}$ cm^2/sn), SF20-I20 ($0.03x10^{-3}$ cm^2/sn), SF40-I30 ($0.08x10^{-3}$ cm^2/sn), SF60-I20 ($0.17x10^{-3}$ cm^2/sn) among their own series. In an experimental study conducted by Mohan and Mini[66], on fresh and mechanical properties of concrete which was obtained with the replacement of cement with silica fume and slag, the addition of 10% silica fume to mixture was reported to exhibit better mechanical and durability properties than other combinations of mixtures.

It was observed that the use of 3% silica fumes in concrete produced by using different subsitution levels of pumice up to 60% besides silica fume up to 9%, showed an excellent behavior in increasing durability and mechanical properties[67]. In general, combinations of silica fume and metal powders at different proportions in mortars showed unpredictable behaviors on mortars. This difference is a direct result of the amount of materials used. Results of the test showed that peak values of sorptivity were obtained at the different percentage of iron powder in mortars own series. In this respect, for instance, SF0-I20 ($0.017x10^{-3}$ cm^2/sn), SF20-I10 ($0.018x10^{-3}$ cm^2/sn), SF40 ($0.03x10^{-3}$ cm^2/sn) and SF60 ($0.11x10^{-3}$ cm^2/sn) have lower sorptivity coefficient compared to their peers in terms of silica fume content.

The addition of silica fume in mixtures increased, sorptivity values at CT-60 and CT-23 curing conditions were gradually becoming closer to each other and curing conditions gradually lost their influence on the durability of geopolymer mortars.

3.2 Mechanical properties

3.2.1 Splitting tensile strength

Splitting tensile strength of mortars is shown in Fig. 7. Results showed that the increment of curing temperature showed good performance with respect to splitting tensile strength, which is one of mechanical

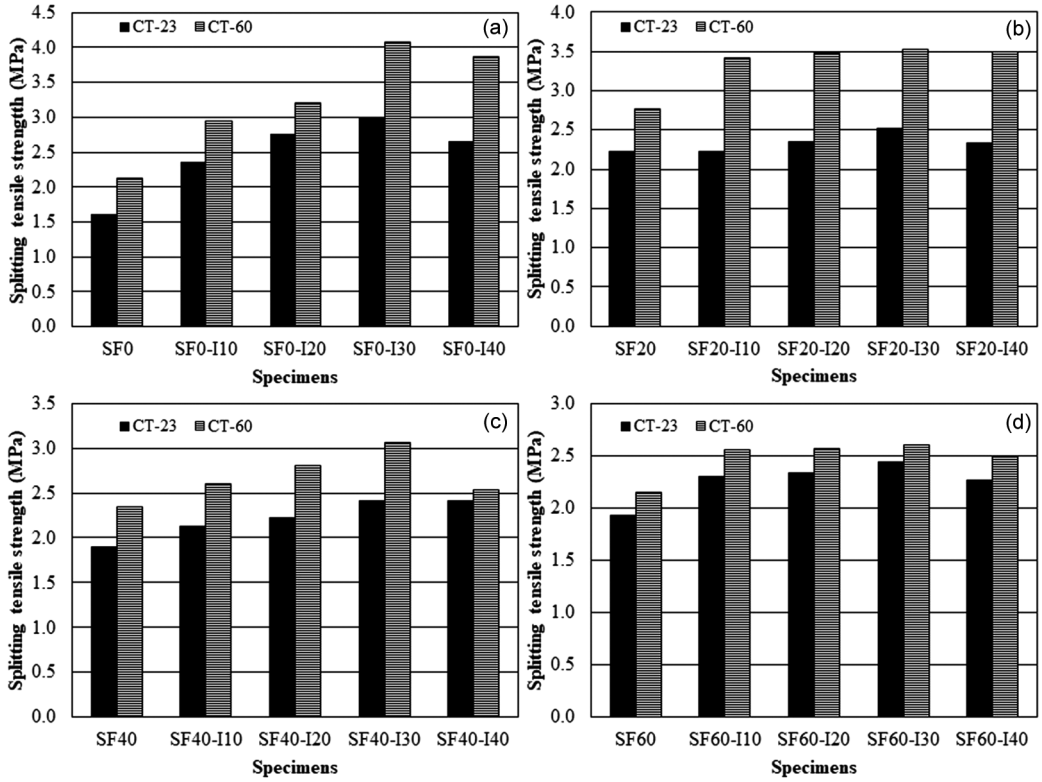

Fig. 7 — Splitting tensile strength for a) SF0-I, b) SF20-I, c) SF40-I, and d) SF60-I series.

properties. Whereas SF0 offered splitting tensile strength of 1.6 MPa at CT-23, it had lower splitting tensile strength of 2.1 MPa at CT-60. Generally, mortars containing up to about 30 percent iron powder by volume of fine aggregates exhibited high performance of splitting tensile strength in typically uses. However, additions of iron powder above 30 percent caused a reduction in splitting tensile strength of mortars. For example, SF0-I30 (4.1 MPa), SF20-I30 (3.5 MPa), SF40-I30 (3.1 MPa), SF60-I30 (2.6 MPa) in their own series had the highest splitting tensile strength at CT-60.

In the study investigating the effect of iron fillings as an alternative to sand in concrete production, it was observed that samples using 100% iron fillings instead of sand caused an increase around 24% in splitting tensile strength, similar to compressive strength compared to control mixtures[68]. It was also confirmed that the splitting tensile strength of 28 days was approximately 9% of the compressive strength for all of samples. Mechanical properties of high-volume iron powder concrete and high-volume fly ash concrete were determined by Han *et al.*[69]. As a result, they stated that high-volume iron powder concrete was found to show lower splitting tensile strength and compressive strength than high-volume fly ash concrete with the same ratio of water/binder. In addition, at CT-60, SF0, SF20, SF40, SF60 were also determined to be have the lowest splitting tensile strength of 2.1 MPa, 2.8 MPa, 2.3 MPa and 2.1 MPa, respectively, among their series. In the study conducted on the effect of adding silica fume and slag on splitting tensile strength of four high-strength concretes, it was reported that mechanical properties of high-strength concretes gave better results by replacing cement with 25% slag and silica fume, by weight[70]. Ghannam *et al.*[71] investigated the splitting tensile strength of concretes produced with partial substitution of the sand used as fine aggregate with iron powder. The researchers stated that increments in tensile strengths of the concrete produced by 5%, 10%, 15% and 20% iron powder replacement compared to the concrete produced without the use of iron powder were observed to be 7.7%, 7.7%, 12.8% and 15.4% respectively.

It was clearly seen that mechanical properties of mortars using iron powder as a partial replacement of fine aggregate significantly increased and a maximum value of splitting tensile strength recorded with the inclusion of 30% iron powder, by volume. The increased iron dosage provided a higher tensile capacity in the tensile direction and splitting tensile strengths were strongly affected by the addition of iron powder in the geopolymer mortar. Nevertheless, silica fume addition of more than 30% to the mix resulted in worse mechanical performance of mortars due to the fact that its large specific surface area typically increased the water demand.

3.2.2 Flexural strength

Figure 8 illustrates effects of silica fume and iron powder additions on flexural strength for different mix ratios and curing periods. In general, flexural strengths of mortars significantly increased with an increase in curing temperature, as was the case with other properties of mortars stated previously. SF0-I40 had flexural strength of 4.1 MPa (CT-23) and 7.0 MPa (CT-60) andit can be said that flexural strength of SF0-I40 mortar increased about 70.7% with the increasing of curing temperature from 23°C to 60°C. Furthermore, the same observation for splitting tensile strength was observed for flexural strength that mortars including 30% iron powder showed the highest flexural strength values. For example, flexural strengths of SF20-I30 and SF40-I30 were 4.6 MPa and 4.9 MPa, respectively, and they showed the highest strength among their series at CT-23. This result shows the positive effect of iron powder aggregate, which has high strength compared to slag aggregate, on flexural strength of mortars. Olutoge *et al.*[72] investigated effects of iron powders used as fine aggregate on the flexural strength of concrete, and the replacement of 10% and 20%, by weight, iron powders with sand compared to the non-iron control mixture was increased flexural strength by 11.1% and 4.8% and then 30% replacement decreased strength by 1.6%. In addition, researchers found that the maximum flexural strength obtained with 10% iron powder substitution was 7.0 N/mm^2.

In order to reduce environmental damages caused by the use of cement, researches were conducted on substitution of pozzolanes as an alternative to cement. According to Moghadam and Izadifard[73], replacing 10% by weight of cement with silica fume increased the tensile strength of normal mortar from 3.35 MPa to 3.46 MPa, with an increase of 3.4%. It was determined that SF60-I40 had a maximum flexural strength of 5.2 MPa (CT-23), considering all mortars. On the other hand, of all mortars produced, SF0 mortar without silica fume and iron powder

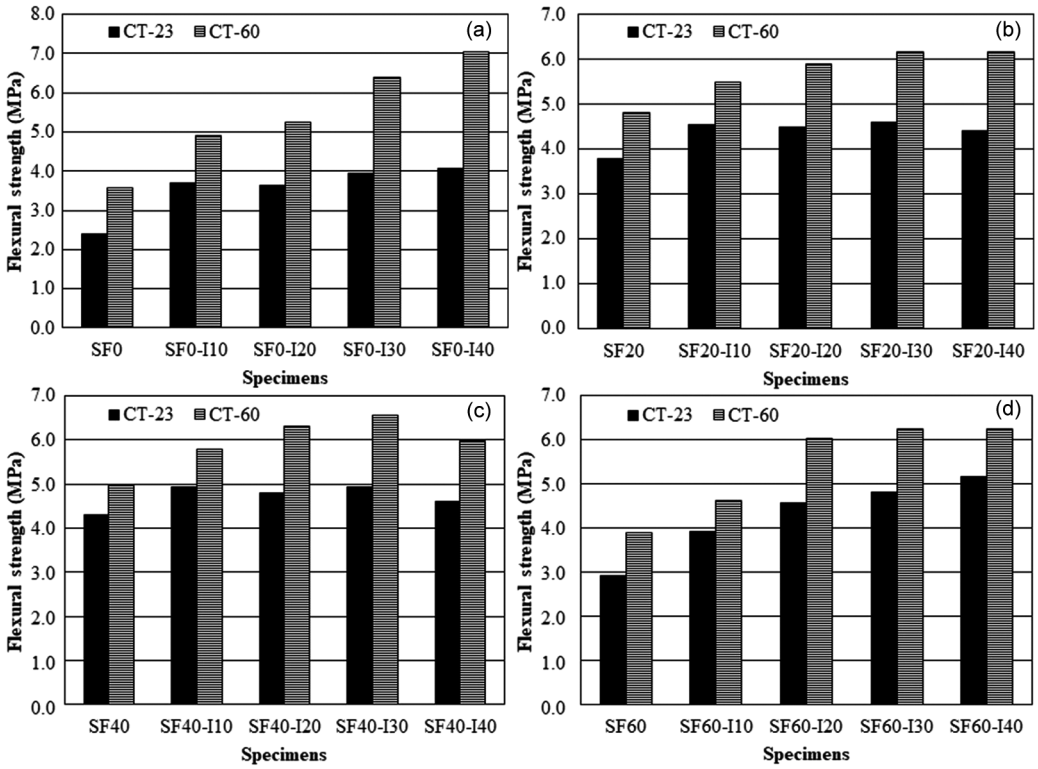

Fig. 8 — Flexural strength for a) SF0-I, b) SF20-I, c) SF40-I, and d) SF60-I series.

replacement exhibited the worst performance with 2.4 MPa flexural strength at CT-23. Based on results of the research carried out by Chaipanich *et al.*[74] on mortars prepared by replacing 10% by weight of cement with silica fume, it was showed that there was an increase in compressive and flexural strength of silica fume based mortars, compared to control mortars without silica fume. This increase in strengths as a result of the use of silica fume was explained by its characteristics such as filling and pozzolanic effects. As a result, iron powder as a partial fine aggregates replacement and silica fume as binder substitution in mortars showed beneficial effects on mechanical properties of mortars.

3.2.3 Compressive strength

Compressive strength tests results are presented in Fig. 9. Maximum values of compressive strength were obtained with 20% replacement by volume of slag with silica fume in mortars. Compressive strengths of these mortars mentioned (SF20) were 41.4 MPa (CT-23) and 52.9 MPa (CT-60). However, these values generally decreased with increasing iron powder content. Results showed that SF20-I40, SF40-I40 ve SF60-I40 indicated the lowest compressive strength by 33.4 MPa, 28.3 MPa and 27.8 MPa, respectively, among their own series at CT-23. In addition, this results also revealed combined effects of adding iron powder along with the silica fume on compressive strength. There was an increment in compressive strength of slag-based mortars with increasing percentage of the iron powder. This can be attributed to a good bond between iron powder and slag-based geopolymer matrix and both iron powder and slag matrix shared loads and this significantly increased the strength of geopolymer mortars. In addition, the performance of iron powder component, which has a filling effect as metal powder, in the direction of fracture with the effect of compression will be much more resistant to the slag aggregate. Han *et al.*[75] observed that precast concrete with 50% iron powder had lower compressive strength than control concrete. However, they stated that in order to remove these negative effects of iron powder on precast concrete properties, iron powder can be partially replaced with slag or fly ash. In addition, it was observed that the effect of the size of iron powder particles on concrete properties was very important and the bond of large particles with hydrates was very weak. In particular, SF0 mortars without iron powders gave the lowest compressive strength by 44.4 MPa, on the contrary,

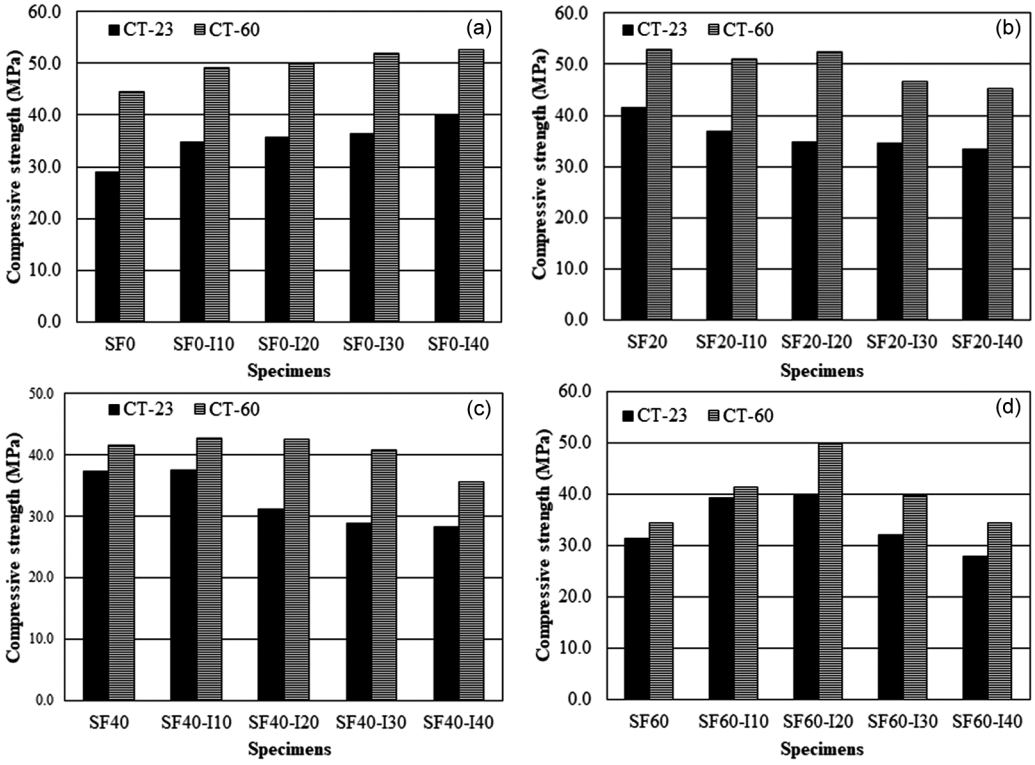

Fig. 9 — Compressive strength for a) SF0-I, b) SF20-I, c) SF40-I, and d) SF60-I series.

SF0-I40 mortars with 40% iron powder substitution showed the highest compressive strength by 52.7 MPa. It can be concluded that behaviors of different materials on mechanical properties were entirely independent from each other. Additionally, to achieve optimum mixture exhibiting best mechanical performance, effects of each materials should be taken into account. Although raw materials forming mixture are increased regularly and gradually, it is not possible to predict how materials will behave. For example, optimum percentage of iron powder to achieve the maximum increase in compressive strength was 20% for SF60 mixture series. The mentioned SF60-I20 was observed to be have compressive strengths by 39.7 (CT-23) and 49.7 MPa (CT-60). Alzaed[76] investigated the possibility of using iron powders as one of components of concrete mixtures.

The researcher examined the effect of iron powders by partial replacement of cementon the compressive strength and observed that the 28-day compressive strength of the sample without iron powder was 27.53 MPa on average, and increases in strengths with the use of 10%, 20% and 30% iron powder were 5.4%, 11.9%, 17.8%, respectively. In the concrete mixes prepared in Portland cement system[77], it was observed the increase of the compressive strength with the increase of the percentage of the waste iron powder, it was also stated that the substitution of 10%, 15%, 20% iron powder instead of the sand used as fine aggregate increased compressive strengths by 8.2%, 15.2% 22.6%, respectively, compared to iron-free reference mixture. Moreover, it can be stated that the slag/silica fume ratio has a threshold value and beyond this critical value, compressive strength will be significantly reduced by increasing the iron powder ratio. Experimental results showed that lower slag/silica fume content leads to higher liquidity. Therefore, excess liquidity can be said to reduce the cohesion of the transition zone and thus it causes a decrease in compressive strength.

The hydration process and the degree of compactness of concrete matrix play an active role in the development of mechanical properties[78]. When compositions of aluminasilicate materials are examined, the slag material has a relatively high CaO content to fly ash[79]. Silica fume, on the other hand, has a high amount of SiO_2 (Table 2). Fly ash and silica fume are mainly composed of spherical particles of different sizes, while slag particles are generally irregular and rough[80-81]. It was determined that microsphere particles in fly ash are much larger than

those in silica fume[82]. This finding indicates that silica fume plays an active role in accelerating strength development of geopolymer composites[83]. The highly active silica, which reacts to consume the excess $Ca(OH)_2$ in the system, provides more C-(A)-S-H gel production, resulting in the formation of a compact microstructure[84-85]. Therefore, the observed increases in strengths of silica fume-containing samples are due to the microstructure becoming denser by filling the internal voids, by ultrafine silica fume particles acting as a microaggregate filler[86]. This result indicates that the limited $Ca(OH)_2$ consumption in fly ash-based compositions is increased by excessive $Ca(OH)_2$ participation to the reaction by breaking the reaction barrier with the addition of highly active silica fume[87]. In different studies in the literature, optimum silica fume content in fly ash-based mixtures was reported as maximum 10%[88]. The optimum silica fume addition level determined in the study investigating engineering properties of sodium carbonate activated fly ash/slag mixed mortars was 4% of the total binder by weight[89]. In the study by Wang *et al.*[90], the percentage of silica fume as the optimum additive with which mechanical properties can be improved in various curing systems was found to be 10% by weight in fly ash-based geopolymer mixtures; this result is due to too much silica tetrahedron derived at silica fume contents beyond 10% attributed to attenuation of geopolymerization. In fly ash-slag-based geopolymers, it was observed that the optimum content for silica fume is 10%[91]. With an increase in silica fume content of more than 10%, large void formations were observed leading to the expansion of samples, resulting in reductions in strength[92]. It was concluded that fly ash-based geopolymers containing 5% micro silica are thermally stable up to 800 °C[93]. As a result, free calcium hydroxide from the slag material, which has a chemical composition closer to cement properties, with a relatively high CaO content to the fly ash, will be consumed with higher percentages of silica fume content during the reaction. Therefore, in this study, 20% silica fume content was determined as the optimum value for improving engineering properties by exceeding the optimum 10% silica fume content, which was emphasized in many studies in the literature. In the study by Lee *et al.*[94], the addition of silica fume caused a decrease in the reactivity of fly ash and an increase in the reactivity of Na in alkali activator and the slag. It was stated that the reactivity of slag, which has a high percentage of Al in its chemical composition, increased as a result of the reaction with the addition of silica fume. It was stated that the reactivity of slag increased with the reaction of Al, which is high percentage in the chemical composition of slag, with silica fume. Similarly, the optimum 20% content of silica fume obtained in this study can be attributed to its reaction with the high Al content originating from slag. Similar to results obtained in this study, test results by Jithendra and Elavenil[95] also report that an increase of up to 20% in silica fume indicates an increase in geopolymer properties.

4 Conclusion

- In all slag/silica fume ratios, oven dry and saturated surface dry bulk density increased almost linearly with the increase of iron powder percentages in mixtures.
- Water absorption and apparent porosity of slag/silica fume based geopolymer mortars increased in parallel with the increase in silica fume content.
- As the percentage of iron powder increased, sorptivity coefficients of mortars subject to CT-23 curing condition showed a downward trend.
- The best splitting tensile strength performance was observed at 30% iron powder substitution for all slag/silica fume ratios.
- Among mortars exposed to CT-23 curing conditions, a maximum flexural strength of 5.2 MPa was obtained with SF60-I40 mortars.
- By replacing the slag volume with 20% silica fume in mortars, a compressive strength of 52.9 MPa (CT-60) was achieved.
- The increasing temperature of water curing from 23°C to 60°C is more effective for the improvement of physical and mechanical properties of geopolymer mortars.

Acknowledgements

This study was financially supported by Akdeniz University Scientific Research Projects Coordination Unit with the number: FDK-2016-1990.

References

1 Visintin P, Mohamed Ali MS, Albitar M, & Lucas W, *Constr Build Mater,* 148 (2017) 10.

2 Kockal NU, Beycan O, & Gulmez N, *Acta Phys Pol A,* 131 (2017) 530.

3 Maheswaran S, Kumar VR, Rehemen MS, Gopinath S, Murthy AR, & Iyer NR, *Indian J Eng Mater Sci,* 24 (2017) 491.

4 Karthik PT, Subramanian K, Jagadesh P, & Nagarajan V, *Indian J Geo-Mar Sci,* 48(11) (2019) 1803.
5 Christy CF, & Tensing D, *Indian J Eng Mater Sci,* 17 (2010) 140.
6 Fanghui H, Xuan Z & Juanhong L, *Indian J Eng Mater Sci,* 27 (2020) 120.
7 He J, Jie Y, Zhang J, Yu Y, & Zhang G, *Cement Concrete Comp,* 37 (2013) 108.
8 Farhana Z F, Kamarudin H, Rahmat A, & Mustafa Al Bakri AM, *Mater Sci Forum,* 803 (2015) 166.
9 Mijarsh MJA, Megat Johari MA, & Zainal Arifin A, *Cement Concrete Comp,* 60 (2015) 65.
10 Wianglor K, Sinthupinyo S, Piyaworapaiboon M, & Chaipanich A, *Appl Clay Sci,* 141 (2017) 272.
11 Kockal NU, Beycan O, & Gulmez N, *Sadhana-Acad P Eng S,* 43 (2018) 1.
12 Subramanian N, & Solaiyan E, *Indian J Eng Mater Sci,* 27 (2020) 67.
13 Tan TH, Mo KH, Ling T, & Lai SH, *Environmental Technology & Innovation*, 18 (2020) 1.
14 Davidovits J, *J Therm Anal*, 35 (1989) 429.
15 Fiset J, Cellier M, & Vuillaume PY, *Cement Concrete Comp,* 110 (2020) 1.
16 Zhao X, Liu C, Wang L, Zuo L, Zhu Q, & Ma W, *Cement Concrete Comp,* 98 (2019) 125.
17 Zawrah MF, Abo Sawan SE, Khattab RM, & Abdel-Shafi AA, *Constr Build Mater,* 246 (2020) 1.
18 Chougan M, Ghaffar SH, Jahanzat M, Albar A, Mujaddedi N, & Swash R, *Constr Build Mater,* 250 (2020) 1.
19 Rashad AM, *Constr Build Mater,* 246 (2020) 1.
20 Kwasny J, Aiken TA, Soutsos MN, McIntosh JA, & Cleland DJ, *Constr Build Mater,* 166 (2018) 537.
21 Alvi MAA, Khalifeh M, & Agonafir MB, *J Petrol Sci Eng,* 191 (2020) 1.
22 Nadoushan MJ, & Ramezanianpour AA, *Constr Build Mater,* 111 (2016) 337.
23 Sun Z, Vollpracht A, & Sloot HA, *Cement Concrete Res*, 125 (2019) 1.
24 Vu MC, Satomi T, & Takahashi H, *Constr Build Mater,* 235 (2020) 1.
25 Alonso MM, Gismera S, Blanco MT, Lanzon M, & Puertas F, *Constr Build Mater*, 145 (2017) 576.
26 Campos HF, Klein NS, & Filho JM, *Materials Research,* 23(5) (2020) e20200285.
27 Chen JJ, Ng PL, Chu SH, Guan GX, & Kwan AKH, *Constr Build Mater,* 252 (2020) 119031.
28 Imam A, Kumar V, & Srivastava V, *Advances in Concrete Construction,* 6(2) (2018) 145.
29 Kwan AKH, & Li LG, *Mater Struct, 45* (2012) 1359.
30 Sanjuan M, Argiz C, Galvez J, & Moragues A, *Constr Build Mater,* 96 (2015) 55.
31 Serelis E., Vaitkevicius V, & Kersevicius V, Chemine Technologija, 67 (2016) 58.
32 Wang FH, & Li S, *Appl Mech Mater,* 238 (2012) 157.
33 Panjehpour M, Ali A, & Demirboga R, *International Journal of Sustainable Construction Engineering and Technology,* 2(2) (2011).
34 Srivastava V, Kumar R, Agarwal V, & Mehta P, *J Environ Nanotechnol,* 3(3) (2014) 32.
35 Duval R, & Kadri E, *Cement Concrete Res,* 28(4) (1998) 533.
36 Xu Y, & Chung D, *Cement Concrete Res,* 29 (1999) 451.
37 Adil G, Kevern J, & Mann D, *Constr Build Mater,* 247 (2020) 118453.
38 Antoni, Chandra L, & Hardjito D, *Procedia Engineering,* 125 (2015) 773.
39 Rostami M, & Behfarnia K, *Constr Build Mater,* 134 (017) 262.
40 Collins F, & Sanjayan JG, *Cement Concrete Res,* 29 (1999) 459.
41 Srinivas T & Ramana Rao NV, *IJRCMCE,* 4(1) (2017) 52.
42 Das SK, Mishra J, Singh SK, Mustakim SM, Patel S, Das SK, & Behera U, *Mater Today - Proc,* (2020) 1.
43 Katpady DN, Takewaka K, Yamaguchi T, & Akira Y, *Constr Build Mater,* 234 (2020) 1.
44 Zhang S, Li VC, & Ye G, *Cement Concrete Comp*, 109 (2020) 1.
45 Zhu H, Liang G, Xu J, Wu Q, & Du J, *Constr Build Mater,* 199 (2019) 574.
46 Guo X, & Yang J, *Constr Build Mater*, 230 (2020) 1.
47 Xiang J, Liu L, He Y, Zhang N, & Cui X, *Cement Concrete Comp,* 99 (2019) 140.
48 Oderji SY, Chen B, Ahmad MR, & Shah SFA, *J Clean Prod*, 225 (2019) 1.
49 Li H, Liu P, Li C, Li G & Zhang H, *Constr Build Mater*, 213 (2019) 20.
50 Shishegaran A, Daneshpajoh F, Taghavizade H, & Mirvalad S, *Constr and Build Mater,* 232 (2020) 1.
51 Kumar EM, & Ramamurthy K, *Constr Build Mater*, 95 (2015) 486.
52 ASTM C 642-06, ASTM International, West Conshohocken, PA, USA, 2006.
53 TS EN 12390-6, TSE, Ankara, Turkey, 2010.
54 TS EN 196-1, TSE, Ankara, Turkey, 2016.
55 TS EN 480-5, TSE, Ankara, Turkey, 2008.
56 Cheah CB, & Ramli M, *American Journal of Applied Sciences,* 8(1) (2011) 82.
57 Miah J, Ali K, Paul SC, Babafemi AJ, Kong SY, & Savija B, *Materials,* 13(5) (2020) 1168.
58 Shettima AU, Hussin MW, Ahmad Y, & Mirza J, *Constr Build Mater,* 120 (2016) 72.
59 Zuccheratte ACV, Freire CB, & Lameiras FS, *Constr Build Mater,* 151 (2017) 859.
60 Yunhong C, Fei H, Shanshan Q, Wenchuan L, Rui L, & Guanglu L, *Constr Build Mater*, 242 (2020) 1.
61 Sasanipour H, Aslani F, & Taherinezhad J, *Constr Build Mater,* 227 (2019) 1.
62 Largeau MA, Mutuku R, & Thuo J, *Open Journal of Civil Engineering,* 8 (2018) 411.
63 Abo Sawan SE, Zawrah MF, Khattab RM, & Abdel-Shafi AA, *Mater Chem Phys,* 239 (2020) 1.
64 Zhao S, Fan J, & Sun W, *Constr Build Mater*, 50 (2014) 540.
65 Adil G, Kevern JT, & Mann D, *Constr Build Mater,* 247 (2020) 1.
66 Mohan A, & Mini KM, *Constr Build Mater,* 171 (2018) 919.
67 Madani H, Norouzifar MN, & Rostami J, *Constr Build Mater,* 174 (2018) 356.
68 Satyaprakash, Helmand P, & Saini S, *Mater Today - Proc,* 15 (2019) 536.
69 Han F, Luo A, Liu J, & Zhang Z, *Constr Build Mater*, 241 (2020) 1.

70 Jianyong L, & Pei T, *Cement Concrete Res,* 27(6) (1997) 833.
71 Ghannam S, Najm H, & Vasconez R, *Sustainable Materials and Technologies,* 9 (2016) 1.
72 Olutoge FA, Onugba MA, & Ocholi A, *British Journal of Applied Science and Technology,* 18(3) (2016) 1.
73 Moghadam MA, & Izadifard RA, *Constr Build Mater*, 253 (2020) 2.
74 Chaipanich A, Rianyoi R, & Nochaiya T, *Mater Today - Proc*, 4 (2017) 6065.
75 Han F, Song S, Liu J, & Huang S, *Powder Technol*, 345 (2019) 292.
76 Alzaed AN, *International Journal of Recent Development in Engineering and Technology,* 3(4) (2014) 121.
77 Ismail ZZ, & AL-Hashmi EA, *Management,* 28 (2008) 2048.
78 Ma Q, & Zhu Y, *Underground Space,* 2 (2017) 175.
79 Puligilla S, & Mondal P, *Cement Concrete Res,* 43 (2013) 70.
80 Matsunaga T, Kim J, Hardcastle S, & Rohatgi P, *Mater Sci Eng, A325* (2002) 333.
81 Blandine A, Essaid B, & Bernard G, *Ceramica, 54* (2008) 388.
82 Chen J, Ng P, Li L, & Kwan A, *Procedia Engineering,* 172 (2017) 165.
83 Wilinska I, & Pacewska B, *J Therm Anal Calorim,* 133 (2018) 823.
84 Cretu A, Mattea C, Stapf S, & Ardelean I, *Molecules,* 25 (2020) 1762.
85 Kansal CM, & Goyal R, *Mater Today - Proc,* 45 (2021) 4520.
86 Mehta A & Ashish DK, *Journal of Building Engineering,* 29 (2020) 100888.
87 Cong P, & Mei L, *Constr Build Mater*, 275 (2021) 122171.
88 Nochaiya T, Wongkeo W, & Chaipanich A, *Fuel, 89* (2010) 768.
89 Cheah CB, Tan LE, & Ramli M, *Compos Part B - Eng,* 160 (2019) 558.
90 Wang YC, Zhang YJ, Xu DL, & Liu LC, *Mater Res Innov,* 17 (2013) 21.
91 Guo X, Yang J, & Xiong G, *Cement Concrete Comp,* 114 (2020) 103820.
92 Sukontasukkul P, Chindaprasirt P, Pongsopha P, Phoo-Ngernkham T, Tangchirapat W, & Banthia N, *Journal of Sustainable Cement-Based Materials,* 9(4) (2020) 218.
93 Sivasakthi M, Jeyalakshmi R, Rajamane N, & Jose R, *J Non-Cryst Solids,* 499 (2018) 117.
94 Lee N, An G, Koh K, & Ryu G, *Adv Mater Sci Eng,* (2016) 2192053.
95 Jithendra C, & Elavenil S, *Silicon,* 12 (2020) 1965.